J Mater Sci (2011) 46:707–714
DOI 10.1007/s10853-010-4798-4

The effect of high-temperature heat-treatment on the strength of C/C–SiC joints

Xiaofei Chen · Shujie Li · Zhijun Chen · Ning Wen

Received: 6 December 2009 / Accepted: 26 July 2010 / Published online: 10 August 2010

Abstract Joining of carbon fiber reinforced C–SiC dual matrix composite (denoted by C/C–SiC) is critical for its aeronautical and astronautical applications. Joining of C/C–SiC has been realized through a reaction joining process using boron-modified phenolic resin with micro-size B_4C and nano-size SiO_2 powder additives. The effect of the heat-treatment temperature on the retained strength of the joints, calculated by dividing the strength of the heat-treated joints by the strength of the joints before heat-treatment, was studied. The maximum retained strength of the joints is as high as 96.0% after the heat-treatment at 1200 °C for 30 min in vacuum, indicating good heat resistance of the joints. The thickness of the interlayer of the joint after the heat-treatment is about 18 μm and it is uniform and densified. There are no obvious cracks or pores at the interfaces. During the heat-treatment, carbon, oxygen, silicon, and boron diffuse at the interfacial area. The interlayer is composed of B_4C, SiO_2, glassy carbon, amorphous B_2O_3, and borosilicate glass. SiC appears in the interlayer of the joint heat-treated at 1400 °C for 30 min in vacuum. The addition of B_4C and SiO_2 powders contributes to the densification of the interlayer, the bonding at the interfaces and the heat resistance of the joints.

X. Chen · S. Li (✉) · N. Wen
School of Materials Science and Engineering, Beijing University of Aeronautics and Astronautics, Beijing 100191, People's Republic of China
e-mail: shujieli@buaa.edu.cn

Z. Chen
Avic Xi'an Aviation Brake Technology Co. Ltd, Xi'an 710075, People's Republic of China

Introduction

Carbon fiber reinforced C–SiC dual matrix composite (denoted by C/C–SiC) is a very promising high-temperature structural material for aeronautical and astronautical applications due to its excellent thermal, physical, and mechanical properties. Joining of C/C–SiC is critical for its extensive applications because the manufacturing of the C/C–SiC parts with large size or complicated shape is difficult and expensive. C/C–SiC is composed of carbon fiber, carbon and SiC dual matrix, hence, joining of C/C–SiC involves joining of carbon fiber, joining of C matrix, joining of SiC matrix, joining of C matrix to SiC matrix, and also joining of carbon fiber exposed on one surface to C and SiC dual matrix on the other. With all the combinations involved, the joining process of C/C–SiC is very complicated. Several joining techniques, such as brazing [1–3], diffusion welding [4, 5], self-propagating high-temperature synthesis welding [6], and reaction joining process [7, 8], have been used to join ceramics and ceramic matrix composites. Among them, the reaction joining process is the most convenient for its wide application and low cost. In this article, we study the joining of C/C–SiC to C/C–SiC through the reaction joining process using the boron-modified phenolic resin (BPF) with B_4C and SiO_2 additives as joining material. The effect of the heat-treatment temperature on the strength and the microstructure of the joints have been investigated.

Experimental procedures

C/C–SiC with density of 1.8 g/cm^3 was used as the base material to be joined, called as substrate in this article. A schematic of the structure of the C/C–SiC is presented in

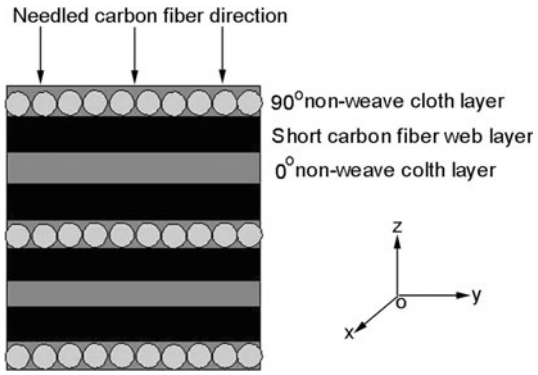

Fig. 1 Schematic of the structure of C/C–SiC

Fig. 1. The C/C–SiC was mechanically machined into cubic billets, with the size of 10 mm × 10 mm × 10 mm. The surfaces for joining were polished with diamond paste with the size of 1.0 μm. Then, the C/C–SiC billets were cleaned with alcohol in an ultrasonic bath for 30 min. BPF with molecular weight of 500 was used as the main component of the adhesive. B_4C powder (the purity of 99.5 wt% and size of 3–5 μm) and SiO_2 powder (the purity of 99.9 wt% and size of 10–30 nm) were used as the additives.

The B_4C and SiO_2 powders were added into the BPF to form a novel high-temperature adhesive. The surface parallel to the needled carbon fiber direction, as shown in Fig. 1, was used as the surface to be joined. The adhesive was brushed onto the surfaces to be joined of the C/C–SiC billets. Then, the C/C–SiC billets and the adhesive were sandwiched between the surfaces to be joined and the whole setup was loaded into a bake oven. A low pressure perpendicular to the surface to be joined was applied on the sample. The C/C–SiC joints were manufactured under the optimized condition that the curing temperature was 200 °C, the curing pressure was 20 kPa, and the curing time was 2 h. Next, the C/C–SiC joints were heated up to five different temperatures, 1000, 1100, 1200, 1300, and 1400 °C in five trials, in vacuum (5×10^{-3} Pa) in a high-temperature furnace. After holding the temperature for 30 min, the samples were furnace-cooled to room temperature.

In the meantime of the joining test and the high-temperature heat-treatment, adhesive identical to that used in joining was placed in a crucible and was processed through the same treatment in the identical equipments. The adhesive after curing under the optimized condition and the pyrolyzates were analyzed with X-ray diffraction (XRD) to determine their phase compositions. In addition, the pyrolyzates were analyzed with infra-red spectroscopy (IR) and X-ray photoelectron spectroscopy (XPS) to investigate their compositions. Thermogravimetry (TG) and differential scanning calorimetry (DSC) analyses were carried out for the adhesive after curing under the optimized condition.

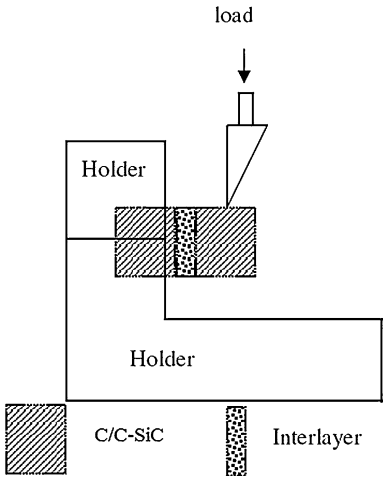

Fig. 2 Schematic of the instrument used to determine join strength

The crystalline phases at the interfacial area of the joint after the heat-treatment at 1200 °C for 30 min in vacuum were identified by grazing incidence XRD. One of the C/C–SiC substrates was removed from the joint by carefully grinding until the interlayer was reached. The C/C–SiC substrate near the interface between the interlayer and the C/C–SiC substrate and the interface were consecutively analyzed by grazing incidence XRD. The X-ray penetration depth for this scan mode was approximately 2 μm.

The size of the obtained joints was 10 mm × 10 mm × (20–20.5) mm. This size is not standard for shearing strength measurement. A special instrument, as shown in Fig. 2, was designed to facilitate the measurement of the join strength. One end of the joint was inserted 9 mm into a holder, and was fixed in place. A load was applied at the position 3 mm away from the interlayer as shown in the figure. This way, the entire welded zone was tested. As can be seen in the figure, the strength measured this way is neither shearing strength, nor bending strength. Nonetheless, it is close to shearing strength. We call it "join strength" in this article.

For comparison purpose, each measurement had to be conducted under identical conditions. The strength of the joints before high-temperature heat-treatment and the strength of the base material C/C–SiC were determined in the same way. Eight specimens were manufactured and examined under the identical conditions. The average value and the statistical uncertainty range of the join strength were calculated for each case. The retained strength of the joints was calculated by dividing the strength of the heat-treated joints by the strength of the joints before the heat-treatment.

The microstructure and the composition of the interfacial area of the joints were determined by electron probe microanalysis (EPMA). The microstructure of the fractures of the joints was observed with a scanning electron microscope (SEM).

Results and discussion

The strength of the base material C/C–SiC determined with the instrument shown in Fig. 2 is 15.3 MPa. The strength of the joints before high-temperature heat-treatment, determined in the same way, is 12.6 MPa. Figure 3 shows the microstructure of the interfacial area of the joint manufactured under the optimized condition. This figure indicates that the thickness of the interlayer is about 20 μm. The interlayer is continuous and basically densified, and the contact at the interfaces is intact with no obvious cracks or pores. It can be seen in the figure that some particles are surrounded by a basically continuous phase in the interlayer. The particles and the basically continuous phase should be B_4C particles and the cured BPF, respectively.

Figure 4 presents the XRD pattern of the adhesive after curing under the optimized condition. A broad diffraction peak at about 23°, is shown in the figure, which can be attributed to the adjacent chains of the cured BPF. Figure 4 demonstrates that the cured adhesive is composed of B_4C, SiO_2, and cured BPF. The BPF possesses outstanding adhesive properties, and the cured BPF with cross-linking net structure has high strength. The joining of the C/C–SiC has been realized by curing reaction of the adhesive under the optimized condition. In the curing process of the adhesive, the B_4C powder additive serves as an inert filler, which can reduce the volume shrinkage of the interlayer, resulting in the decrease of the stress of the joints. In the meantime, the particle reinforcement of the particulate additives improves the mechanical properties of the interlayer. Moreover, H-bonding force between the BPF matrix and the nano-size SiO_2 can be formed due to the active Si–OH function group on the surface of the nano-size SiO_2 [9], which contributes to enhancement of the cohesive force of the interlayer.

Figure 5 shows the effect of the heat-treatment temperature on the retained strength of the C/C–SiC joints. It can be seen in the figure that the retained strength of the joints increases as the heat-treatment temperature increases until it reaches the maximum of 96.0% at 1200 °C, indicating good heat resistance of the joints, and it decreases as the heat-treatment temperature further increases to 1400 °C. Measured the same way, the maximum strength of the joints heat-treated at 1200 °C is determined to be 12.1 MPa, which is equal to 79.1% of the strength of the base material C/C–SiC.

Figure 6 shows the XRD pattern of the pyrolyzate of the adhesive after the heat-treatment at 1200 °C for 30 min in vacuum. This figure indicates that the pyrolyzate is composed of B_4C, SiO_2, and glassy carbon, among which B_4C and SiO_2 are the remainders of the additives in the adhesive, and glassy carbon should be the product of pyrolysis of phenolic resin [10]. The figure also shows that the diffraction peaks of glassy carbon are strong.

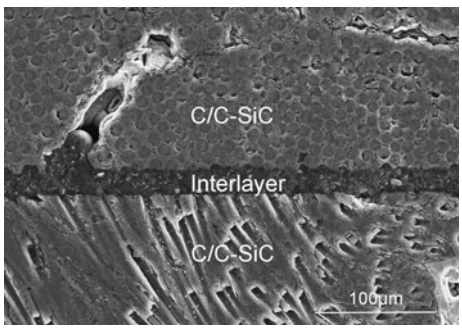

Fig. 3 The microstructure of the interfacial area of the joint manufactured under the optimized condition

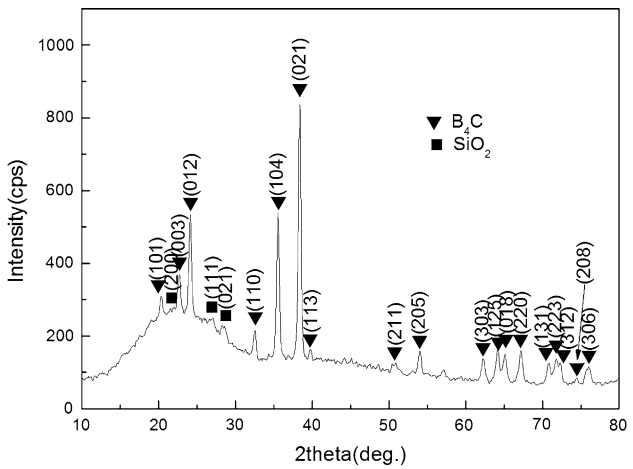

Fig. 4 The XRD pattern of the adhesive after curing under the optimized condition

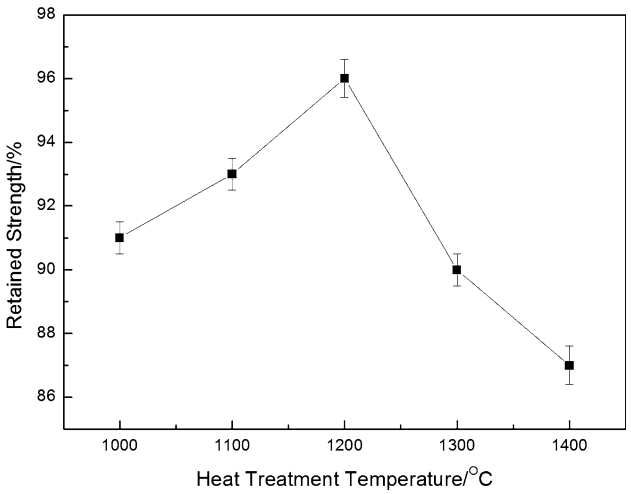

Fig. 5 The effect of the heat-treatment temperatures on the retained strength of the joints with the holding time of 30 min in vacuum

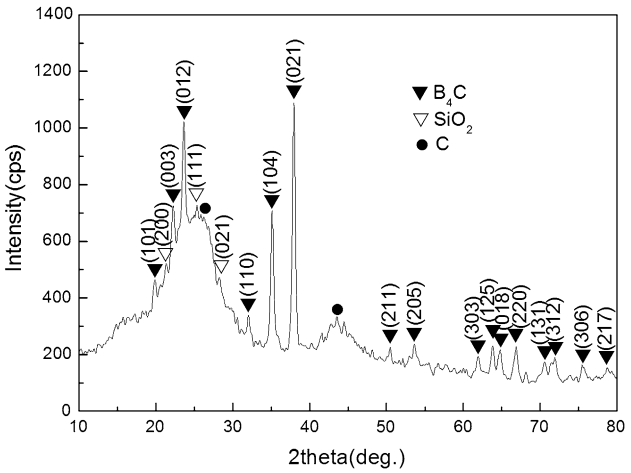

Fig. 6 The XRD pattern of the pyrolyzate of the adhesive after the heat-treatment at 1200 °C for 30 min in vacuum

Figure 7 shows the XRD pattern of the pyrolyzate of the adhesive after the heat-treatment at 1400 °C for 30 min in vacuum. It can be seen in the figure that SiC appears in the pyrolyzate besides B_4C, SiO_2, and glassy carbon, which also appear in Fig. 6. The formation of SiC could be attributed to the following reaction [11]:

$$SiO_2(s) + 3C(s) = SiC(s) + 2CO(g). \quad (1)$$

This reaction consumes the glassy carbon and results in the decrease of the glassy carbon content of the pyrolyzate. One can also see that the diffraction peaks of glassy carbon in Fig. 7 are much weaker than those in Fig. 6, although both of them were analyzed under the identical conditions. This result could be an evidence to support that the glassy carbon content in the joint heat-treated at 1400 °C is much less than that in the joint heat-treated at 1200 °C.

Figure 8 presents the XPS B 1s spectrum of the pyrolyzate of the adhesive after the heat-treatment at 1300 °C

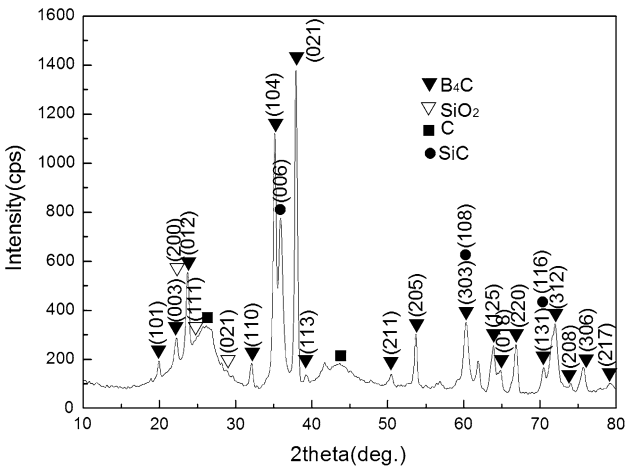

Fig. 7 The XRD pattern of the pyrolyzate of the adhesive after the heat-treatment at 1400 °C for 30 min in vacuum

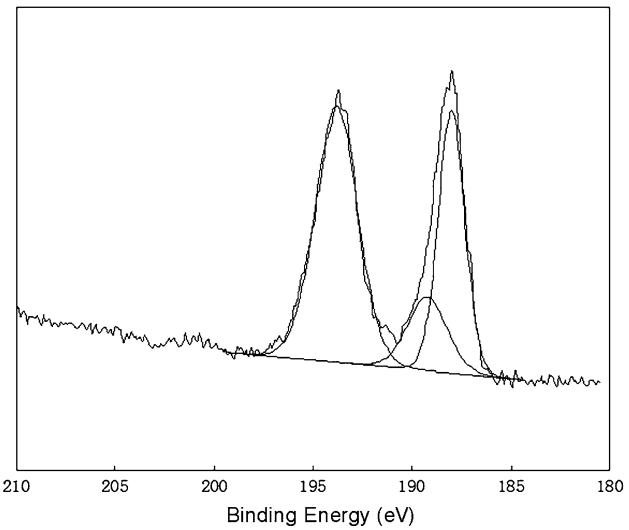

Fig. 8 The XPS B 1s spectrum of the pyrolyzate of the adhesive after the heat-treatment at 1300 °C for 30 min in vacuum

for 30 min in vacuum. One can see in the figure that there are three component peaks with various intensities in the spectrum. The component at the binding energy 187.99 eV can be attributed to B–C bond in the B_4C [12], and the component at 189.21 eV can be attributed to the BC_2O [13]. The component at the highest binding energy 193.81 eV should be due to the presence of oxide. Therefore, the peak at 193.81 eV should correspond to B_2O_3 glass. This result can be explained as the following: In the high-temperature heat-treatment process, the B_4C additive is oxidized into B_2O_3, then, the B_2O_3 melts and forms a structure of glassy phase. In this structure, the boron atoms exist in $[BO_3]$ triangle, resulting in the increase of the binding energy of B 1s. The Fig. 8 also shows that the contents of the components at 187.99, 189.21, and 193.81 eV are 40.53, 14.00, and 45.47%, respectively.

Figure 9a is the IR spectrum of the pyrolyzate of the adhesive after the heat-treatment at 1200 °C for 30 min in vacuum. Figure 9b presents the IR spectrum of the B_4C additive analyzed under the identical condition. Comparing Fig. 9a with Fig. 9b, one can see that the peaks at 1565, 1417, 1086, 843, 703, and 605 cm^{-1} in Fig. 9a are attributed to characteristic absorption of the B_4C. The peak appearing at 1336 cm^{-1} in Fig. 9a is the characteristic peak of B_2O_3. This result demonstrates that a part of the B_4C additive has been oxidized into B_2O_3, which exists in the interlayer. The peak at 951 cm^{-1} in Fig. 9a is the characteristic peak of B–O–Si bond, which indicates that a part of the SiO_2 additive has reacted with the B_2O_3, resulting in the formation of borosilicate in the interlayer. This result is in accordance with that reported in Ref. [14]. In addition, Fig. 9a shows that the peaks at 1071 and 475 cm^{-1} appear, which are attributed to the Si–O–Si bond, indicating the existence of SiO_2 in the interlayer.

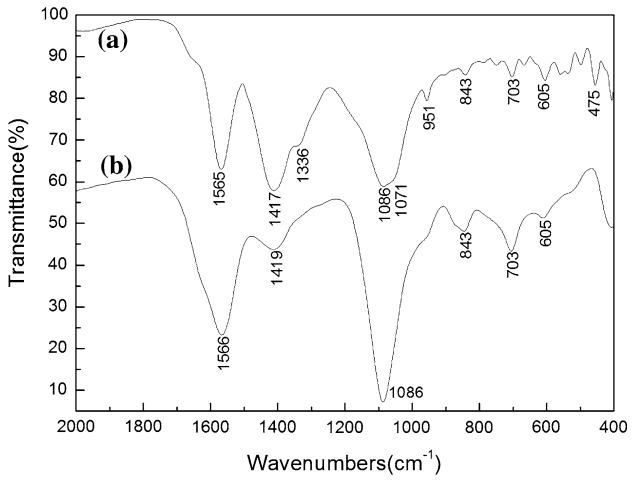

Fig. 9 The IR spectra of the pyrolyzate of the adhesive after the heat-treatment at 1200 °C for 30 min in vacuum (**a**) and the B_4C (**b**)

In the high-temperature heat-treatment, the products of the decomposition of phenolic resin provide an oxidizing atmosphere. The oxidizing volatiles could oxidize B_4C into B_2O_3 at temperatures of 500–600 °C [15]. In the oxidation reaction of B_4C, some volatile components, such as CO and H_2O, react with B_4C, leading to the formation of carbon, which remains in the interlayer. The chemical reactions are listed as the following [16]:

$$B_4C\ (s) + 6CO\ (g) = 2B_2O_3(1) + 7C\,(s), \quad (2)$$

$$B_4C\ (s) + 6H_2O\,(g) = 2B_2O_3(1) + C\,(s) + 6H_2\,(g). \quad (3)$$

In view of the fact that the diffraction peaks of B_2O_3 and borosilicate do not appear in the XRD patterns shown in Figs. 6 and 7, one can infer that the B_2O_3 and the borosilicate in the pyrolyzates of the adhesive are amorphous.

As reported in [17], the satisfactory wetting ability of ropy liquid B_2O_3 on carbon contributes to the enhancement of the interfacial bonding force between the interlayer and the C/C–SiC substrate. In addition, the conversion of B_4C into B_2O_3 can result in 250% volume increase [16], contributing to the densification of the interlayer, besides, it leads to the reduction of the volume shrinkage of the interlayer, and consequently the decrease of the residual stress in the joints, contributing to the enhancement of join strength. The B_2O_3 content in the interlayer increases with the increasing of the heat-treatment temperature within a certain temperature range. The increase of the B_2O_3 content contributes to the enhancement of the interfacial bonding force between the interlayer and the C/C–SiC substrate, and to the decrease of the residual stress in the joints. Hence, the increasing of the heat-treatment temperature can result in the increase of the retained strength of the joints as shown in Fig. 5 below 1200 °C.

The pyrolysis of phenolic resin leads to the formation of glassy carbon and consequently the formation of an integrated glassy carbon structure, which possesses high strength, at appropriate pyrolysis temperature [18]. As shown in Fig. 6, the diffraction peaks of the glassy carbon are strong. Also taking into account that the retained strength of the joints reaches its maximum at 1200 °C, as shown in Fig. 5, one can infer that an integrated glassy carbon structure may form in this joint.

When the heat-treatment temperature reaches 1200 °C, SiO_2 reacts with B_2O_3 to form borosilicate glass, which inhibits the volatilization of B_2O_3 and prevents glassy carbon from reacting with SiO_2 or B_2O_3, contributing to enhancement of the stability and density of the interlayer. In addition, since the stability, viscosity, and heat resistance of borosilicate glass are higher than those of the B_2O_3 glass [19], the formation of borosilicate glass improves the cohesive strength of the interlayer at high temperatures. This is also a reason for the retained strength of the joints to reach its maximum at the heat-treatment temperature of 1200 °C.

When the heat-treatment temperature reaches 1400 °C, as shown in Fig. 7, the brittle SiC phase forms. The presence of brittle SiC weakens the mechanical properties of the interlayer. Furthermore, the content of glassy carbon in the joint is much less than that in the joint heat-treated at 1200 °C, indicating that the integrity of the glassy carbon structure, existing in the joint heat-treated at 1200 °C, has been partially destroyed, coinciding with the formation of SiC. Therefore, the retained strength of the joints heat-treated at 1400 °C is much lower than that at 1200 °C, as shown in Fig. 5.

Figure 10 shows the TG and DSC curves obtained at the heating rate of 10 °C/min and the argon flow rate of 50 mL/min for the adhesive after curing under the optimized condition. It can be seen in the figure that, below 400 °C, the mass of the sample decreases slowly as the temperature increases. The mass loss in this stage is about 5%, which is due to the evaporation of some small molecules originally adsorbed, such as N_2, O_2, and H_2O etc. In the temperature range of 400–800 °C, the mass of the sample decreases rapidly with the increasing of the

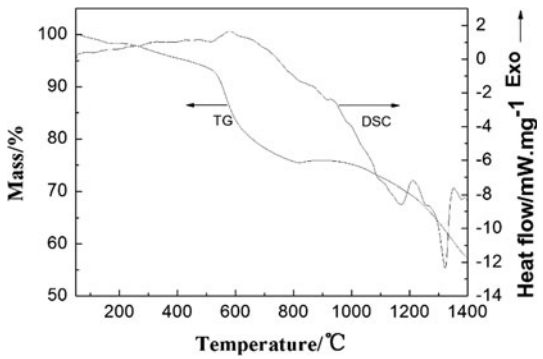

Fig. 10 The TG and DSC curves of the cured adhesive with the heating rate of 10 °C/min and the Ar flow rate of 50 mL/min

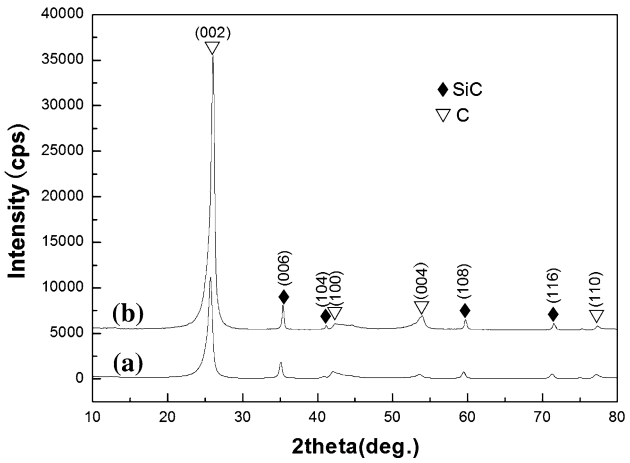

Fig. 11 The grazing incidence XRD patterns of the interface between the interlayer and the C/C–SiC substrate (**a**) and the C/C–SiC substrate (**b**) of the joint after the heat-treatment at 1200 °C for 30 min in vacuum

temperature. The mass loss in this stage is about 20%, which can be attributed to the pyrolysis of the BPF and the consequent volatilization of the volatile pyrolytic products such as CO, CO_2, and H_2O etc. The pyrolysis is an exothermal reaction, which is in accordance with the exothermal peak of the DSC curve in this temperature range. In the temperature range of 1000–1400 °C, the mass loss of the sample is about 17%. The DSC curve shows that there is an exothermal peak around 1200 °C, which should be due to the further decomposition of BPF and the accompanied exothermal effect [20]. With regard to the exothermal peak appearing around 1350 °C in the DSC curve, it can be explained by the formation of SiC as shown in Fig. 7, and the consequent partial disintegration of the glassy carbon structure.

In order to investigate the interfacial reaction of the joint in the heat-treatment at 1200 °C for 30 min in vacuum, the interface between the interlayer and the C/C–SiC substrate of the joint after the heat-treatment was analyzed with grazing incidence XRD. Its XRD pattern is presented in Fig. 11a. The C/C–SiC substrate near the interface was also analyzed in the same way under the identical condition. Its XRD pattern is shown in Fig. 11b. One can see in Fig. 11 that both the interface and the substrate are composed of SiC and C. In order to compare the intensity of SiC diffraction peak of the interface with that of the substrate, we calculated the relative intensity of SiC diffraction peak by dividing the intensity of the characteristic diffraction peak of SiC, SiC(006), by the intensity of the characteristic diffraction peak of C, C(002), of the same pattern. The result shows that the relative intensity of SiC diffraction peak of the interface is stronger than that of the substrate, which can be an evidence to support that the SiC content at the interface is more than that in the substrate, implying that new SiC forms at the interface.

The EPMA micrograph of the interfacial area of the joint manufactured under the optimized condition and after the heat-treatment at 1200 °C for 30 min in vacuum is presented in Fig. 12a. This photograph shows that the interlayer with a thickness of about 18 μm is uniform and densified. The contact at the interfaces is intact with no obvious cracks or pores. Moreover, the adhesive infiltrates into the micropores of the C/C–SiC substrate, as shown in the regions marked by the black letters A, B, and C, which contributes to the enhancement of the join strength. The line distributions of the elements C, O, Si, and B along the analysis line at the interfacial area of the joint are shown in Fig. 12b. This figure demonstrates that the distributions of the elements in the interlayer are uniform, also the tendencies of O line, Si line, and B line are raising along the analysis line from the substrate to the interlayer. The inclination of the distribution lines of the elements at the interfacial area indicates that C, O, Si, and B diffuse at this area, among which O, Si, and B diffuse from the interlayer into the C/C–SiC substrate. These diffusions contribute to the interfacial bonding. As Si diffuses from the interlayer into the substrate in the heat-treatment, it may react with C in the substrate to form SiC. Since the Si content at the interface is more than that in the substrate, as shown in Fig. 12b, the content of the formed SiC at the interface should be more than that in the substrate. This can be another evidence to support that the SiC content at the interface is more than that in the substrate, as discussed with Fig. 11 in the last paragraph. The interfacial reaction can enhance the interfacial bonding force and consequently improve the join strength.

Figure 13 is the SEM micrograph of the fracture surface of the joint manufactured under the optimized condition and after the heat-treatment at 1200 °C for 30 min in vacuum. This photograph indicates that the fracturing takes place in the interfacial area, some fibers in the C/C–SiC substrate have been pulled out from the billet, and some C–SiC matrices extracted from the other side still adhere to the interlayer. These results demonstrate that the fracture surface is in a mixed-mode, which indicates good wetting ability of the system and a sound bonding between the C/C–SiC substrate and the interlayer.

Conclusions

The retained strength of the joints increases with the increasing of the heat-treatment temperature and reaches the maximum of 96.0% at 1200 °C, then, it decreases with the further increasing of the temperature. These results indicate that the joints possess good heat resistance.

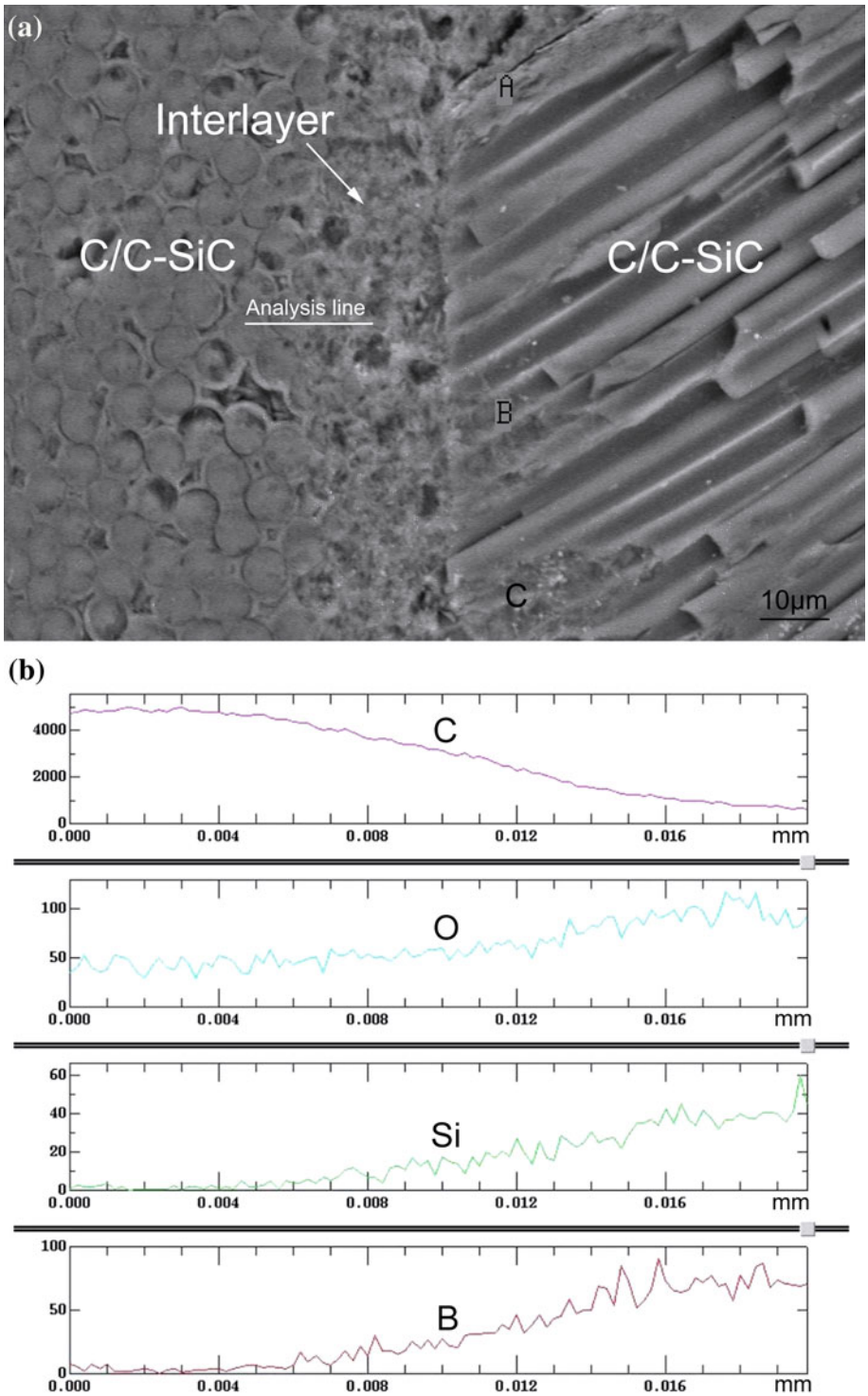

Fig. 12 The EPMA micrograph and the line distributions of the elements along the analysis line at the interfacial area of the joint manufactured under the optimized condition and after the heat-treatment at 1200 °C for 30 min in vacuum

The TG and DSC curves of the adhesive show that the mass loss of the adhesive between 50 and 1400 °C is about 42%. The mass loss happens mainly in the temperature ranges of 400–800 and 1000–1400 °C, which is in accordance with the exothermal peaks of the DSC curve, corresponding to pyrolysis of the adhesive and the reaction to form SiC.

Microstructural study and phase analysis reveal that the thickness of the interlayer of the joints after the heat-treatment at 1200 °C for 30 min in vacuum is about 18 μm, and the interlayer is uniform and densified. The distributions of the elements C, O, Si, and B in the interlayer are uniform. During the heat-treatment, C, O, Si, and B diffuse at the interfacial area, contributing to the interfacial

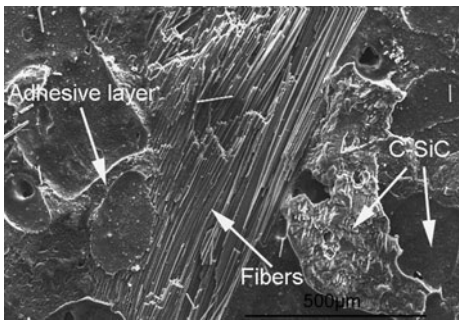

Fig. 13 The SEM micrograph of the fracture surface of the joint manufactured under the optimized condition and after the heat-treatment at 1200 °C for 30 min in vacuum

bonding. The interlayer is composed of B_4C, SiO_2, glassy carbon, amorphous B_2O_3, and borosilicate glass. SiC appears in the interlayer of the joint heat-treated at 1400 °C for 30 min in vacuum.

The B_4C and SiO_2 powder additives in the adhesive contribute to the densification of the interlayer, the bonding at the interfaces, and the heat resistance of the joints.

Acknowledgement The authors gratefully acknowledge the financial support of the project by the National Natural Science Foundation of China (grant no. 50974008).

References

1. Asthana R, Singh M (2008) J Eur Ceram Soc 28:617
2. Asthana R, Singh M (2009) Scr Mater 61:257
3. Shirzadi AA, Zhu Y, Bhadeshia HKDH (2008) Mater Sci Eng A 496:501
4. Mustafa A (2008) J Fac Eng Archit Gazi Univ 23:595
5. Halbig MC, Singh M, Shpargel TP, Kiser JD (2006) Ceram Eng Sci Proc 27:133
6. Li SJ, Duan HP, Liu S, Zhang YG, Dang ZJ, Zhang Y, Wu CG (2000) Int J Refract Met Hard Mater 18:33
7. Lu YW, Zhang YD, Hu HF, Zhang CR (2008) Key Eng Mater 368–372:1044
8. Li SJ, Liu WH, Lu YK, Li XG, Mao YW (2008) Acta Mater Compos Sin 25:72
9. Hernández-Padrón G, Rojas F, Castaño V (2006) Surf Coat Technol 201:1207
10. Abidzina V, Tereshko I, Elkin I, Muntele I, Muntele C, Minamisawa RA (2007) Methods Phys Res Sect B 257:523
11. Gadiou R, Serverin S, Gibot P, Vix-Guterl C (2008) J Eur Ceram Soc 28:2265
12. Cermignani W, Palulson TE, Onneby C, Pantano C (1995) Carbon 4:367
13. Jacques S, Guette A, Bourrat X, Langlais F, Guimon C, Labrugere C (1996) Carbon 9:1135
14. Trick KA, Saliba TF (1995) Carbon 11:l509
15. Wang JG, Jiang N, Guo QG, Liu L, Song JR (2006) J Nucl Mater 348:108
16. Sheehan JE (1989) Carbon 27:709
17. Wang JG, Jiang N, Jiang HY (2006) Int J Adhes Adhes 26:532
18. Myalski J, Sleziona J (2006) J Mater Process Technol 175:291
19. Cheng LF, Xu YD, Zhang LT, Yin XW (2002) J Mater Sci 37:5339. doi:10.1023/A:1021089411141
20. Wang DC, Chang GW, Chen Y (2008) Polym Degrad Stab 93:125